Cerebral Cortex, 2020;00: 1–10

doi: 10.1093/cercor/bhaa328
Original Article

ORIGINAL ARTICLE

Intergenerational Transmission of Cortical Sulcal Patterns from Mothers to their Children

Banu Ahtam[1,2], Ted K. Turesky[2,3], Lilla Zöllei[4], Julianna Standish[1], P. Ellen Grant[1,2], Nadine Gaab[2,3] and Kiho Im[1,2]

[1]Fetal-Neonatal Neuroimaging & Developmental Science Center, Division of Newborn Medicine, Department of Pediatrics, Boston Children's Hospital, Boston, MA 02115, USA, [2]Harvard Medical School, Department of Pediatrics, Boston, MA 02115, USA, [3]Laboratories of Cognitive Neuroscience, Division of Developmental Medicine, Department of Medicine, Boston Children's Hospital, Boston, MA 02115, USA and [4]A.A. Martinos Center for Biomedical Imaging, Department of Radiology, Massachusetts General Hospital, Boston, MA 02129, USA

Address correspondence Kiho Im, PhD, Boston Children's Hospital, 300 Longwood Avenue, Boston, MA 02115, USA. Email: Kiho.Im@childrens.harvard.edu; Banu Ahtam, DPhil, Boston Children's Hospital, 300 Longwood Avenue, Boston, MA 02115, USA. Email: Banu.Ahtam@childrens.harvard.edu.

Abstract

Intergenerational effects are described as the genetic, epigenetic, as well as pre- and postnatal environmental influence parents have on their offspring's behavior, cognition, and brain. During fetal brain development, the primary cortical sulci emerge with a distinctive folding pattern that are under strong genetic influence and show little change of this pattern throughout postnatal brain development. We examined intergenerational transmission of cortical sulcal patterns by comparing primary sulcal patterns between children ($N = 16$, age 5.5 ± 0.81 years, 8 males) and their biological mothers ($N = 15$, age 39.72 ± 4.68 years) as well as between children and unrelated adult females. Our graph-based sulcal pattern comparison method detected stronger sulcal pattern similarity for child–mother pairs than child-unrelated pairs, where higher similarity between child–mother pairs was observed mostly for the right lobar regions. Our results also show that child–mother versus child-unrelated pairs differ for daughters and sons with a trend toward significance, particularly for the left hemisphere lobar regions. This is the first study to reveal significant intergenerational transmission of cortical sulcal patterns, and our results have important implications for the study of the heritability of complex behaviors, brain-based disorders, the identification of biomarkers, and targets for interventions.

Key words: brain development, cortical folding, intergenerational transmission, magnetic resonance imaging, sulcal pattern

Introduction

Parents have a substantial genetic, epigenetic, as well as pre- and postnatal environmental influence on their offspring's behavior, cognition, and brain development known as intergenerational effects (Yamagata et al. 2016). The unique contribution from mothers and fathers to the development of their offspring shows differential influence, called parent-of-origin effects (Curley and Mashoodh 2010). Intergenerational transmission of traits from parent to child have been mostly studied for psychiatric disorders such as depression (Thompson et al. 2014; Yamagata et al. 2016), generalized anxiety disorder (Aktar et al. 2017), conduct problems (D'Onofrio et al. 2007), posttraumatic stress disorder (Yehuda et al. 2005), and maternal adverse experiences during childhood (Yehuda et al. 2016; Moog et al. 2018). There has been extensive work on identifying risk genes for complex behaviors, such as depression and anxiety, in humans, which show that such behaviors are in part heritable (Ho et al. 2016). Effects of genetics and epigenetics occur at a molecular level and are not easy to relate to complex behavior (Flint et al. 2014; Ho et al. 2016). On the other hand, studying endophenotypes at the level of brain structure bridges the gap between genetics and clinical symptoms (Flint et al. 2014; Ho et al. 2016).

Studying the intergenerational transmission of brain structure and function between parents and their offspring helps us learn more about the heritability of complex behaviors, brain-based disorders, the identification of possible biomarkers, and targets for interventions (Ho et al. 2016).

There is limited research on the neural basis of intergenerational effects in humans. It has been observed that the regional gray matter volume in the corticolimbic circuitry (i.e., amygdala, hippocampus, and prefrontal cortex), which is involved in mood regulation and depression, shows a matrilineal transmission pattern, showing a strong association between mothers and daughters (Yamagata et al. 2016). The association between mothers and daughters were stronger compared to mother–son, father–daughter, and father–son pairs (Yamagata et al. 2016). Another study has shown that maternal childhood maltreatment was associated with lower intracranial volume of the newborn children of these mothers, suggesting that the childhood maltreatment effects may be transmitted across generations and that these effects may have originated during the intrauterine life (Moog et al. 2018). Furthermore, thinner cortical gray matter has been reported in depressed mothers and their high-risk daughters compared to nondepressed mothers and their low-risk daughters, suggesting that some heritable disorders also transmit neuroanatomical vulnerability factors from parents to their high-risk children (Foland-Ross et al. 2016).

The in utero development of the human brain is influenced by environment, genetics and epigenetics, which have a significant impact on life-long consequences (Kochunov et al. 2010). Most of the cortical folding happens during fetal brain development, particularly between gestational weeks 20 and 35 where the brain transforms from a smooth to a convoluted surface with gyri and sulci (Garel et al. 2003). During this process, the primary cortical sulci emerge with a distinctive folding pattern that are under strong genetic influence and there is little change of this pattern throughout postnatal brain development (Garel et al. 2001; Rakic 2004; Kostovic and Vasung 2009; Hill et al. 2010; Meng et al. 2014; Rash and Rakic 2014; Sun and Hevner 2014; de Juan Romero et al. 2015; Cachia et al. 2016; Le Guen, et al. 2018a). Furthermore, there are studies that show heritability for the asymmetry of the superior temporal sulcus which could be related to language lateralization (Le Guen, et al. 2018a; Le Guen, et al. 2018b). In addition, heritable brain features with respect to aging, cortical atrophy, and cognitive decline, have also been shown (Le Guen et al. 2019). The global pattern of the sulci, namely the positioning, arrangement, number, and the size of sulcal pits and folds, as well as their intersulcal relationships, is hypothesized to be related to the optimal organization of cortical functional areas and underlying white matter connectivity (Van Essen 1997; Klyachko and Stevens 2003; Rakic 2004; Fischl et al. 2008; Im et al. 2010; Im, et al. 2011a; Sun and Hevner 2014). Since the primary cortical sulcal patterns are determined prenatally under strong genetic control and are associated with cortical functions, studying sulcal patterns across generations can give us a better understanding of intergenerational transmission of brain structure and its associated behavioral phenotype.

In our previous study, we developed a comprehensive and quantitative sulcal pattern analysis technique using a graph structure that completely characterizes the geometric and topological pattern of the primary cortical folds (Im, et al. 2011b). This method has provided a quantification of atypical sulcal folding patterns in patients with polymicrogyria (Im, et al. 2013b), developmental dyslexia (Im et al. 2016), and congenital heart disease (Morton et al. 2019). In addition to these developmental disorders, we have studied sulcal patterns in monozygotic twins where we showed that the similarity of the sulcal patterns of both hemispheres and all lobar regions in twin pairs was significantly higher compared to the similarity between unrelated pairs, supporting a genetic influence on sulcal patterning (Im, et al. 2011b). However, since twin studies often do not collect parental brain data, they cannot directly help with the assessment of intergenerational effects.

The aim of the current study was to first examine intergenerational transmission of cortical sulcal patterns by comparing primary sulcal patterns between children and their mothers as well as between children and unrelated adult females. We hypothesized that there would be a stronger similarity in sulcal patterns between children and their biological mothers compared to the similarity between children and unrelated female adults. Because there have been studies showing different associations between mothers and daughters compared to mothers and sons (Yamagata et al. 2016), and that some disorders and traits are more heritable in females than in males (Sandin et al. 2017), we also expected to see differences in the intergenerational transmission of sulcal patterns between the daughter–mother versus son–mother pairs.

Materials and Methods

Participants

Data from 31 individuals, specifically, 15 adult females (age [mean ± SD]: 39.72 ± 4.68 years) and their 16 children (8 sons, 8 daughters) (age: 5.5 ± 0.81 years) were analyzed in this study. The mean age for daughters was 5.30 ± 0.73 years and the mean age for sons was 5.69 ± 0.89 years. All mothers had one participating child, except for one mother who had 2 daughters participating in the study. Participant characteristics are reported in Table 1. Participants were recruited from the greater Boston community. All participants were administered the Kaufman Brief Intelligence Test—Second Edition (KBIT-2) and had average or above average nonverbal IQ. Daughters and sons were matched on age and nonverbal IQ measured at the age of 4 years. Participants were healthy individuals, without history of neurological trauma, brain surgery, claustrophobia, any metallic implants, or any other contraindications to magnetic resonance imaging (MRI) scanning. This study was approved by the Institutional Review Board of Boston Children's Hospital and written consent for participation in the study was provided by parents for themselves and for their children.

MRI Acquisition

MRI data were collected at Boston Children's Hospital with a 3 T Siemens scanner (32-channel head coil). Participants were not sedated for the scan. The structural sequence was a T1-weighted magnetization-prepared rapid-acquisition gradient-echo with prospective motion correction (mocoMEMPRAGE) acquisition with repetition time (TR) = 2520 ms, echo time (TE) = 1.73–1.75 ms, inversion time (TI) = 1450 ms, flip angle = 1–7°, and voxel size (mm) = 1.0 × 1.0 × 1.0. Children were scanned with field of view (FOV) = 216 mm and 160 sagittal slices and mothers were scanned with FOV = 256 mm and 176 sagittal slices.

Table 1 Participant characteristics

Participant	Group	Age (years)	Nonverbal IQ score
child_01	Daughter	5.08	113
child_02	Daughter	5.08	124
child_03	Daughter	4.67	104
child_04	Son	5.08	110
child_05	Daughter	4.92	85
child_06	Daughter	6.83	94
child_07	Son	6.75	100
child_08	Son	6.75	99
child_09	Daughter	5.00	101
child_10	Son	5.75	121
child_11	Son	4.83	118
child_12	Daughter	4.83	107
child_13	Daughter	6.00	115
child_14	Son	5.25	110
child_15	Son	6.58	99
child_16	Son	4.58	105
mother_01	Mother	37.25	130
mother_02	Mother	46.58	128
mother_03	Mother	38.08	130
mother_04	Mother	38.92	130
mother_05	Mother	30.75	102
mother_06	Mother	32.42	109
mother_07	Mother	40.58	102
mother_08	Mother	43.33	132
mother_09	Mother	35.08	98
mother_10	Mother	42.17	130
mother_11	Mother	38.33	125
mother_12	Mother	44.33	115
mother_13	Mother	46.00	102
mother_14	Mother	38.92	120
mother_15	Mother	43.08	109

Data Processing and Quantitative Similarity Measurement of Sulcal Pattern

In order to perform sulcal pattern analysis for adult and child data, structural T1-weighted images were processed and cortical surfaces were reconstructed using the FreeSurfer software (Fischl 2012). The quality of the Freesurfer segmentation was evaluated with the Qoala-T software (Klapwijk et al. 2019) as well as visually and the quality of white/gray matter boundary of the surface (inner cortical surface) was evaluated visually. Then, the inner cortical surfaces were automatically parcellated into frontal, parietal, temporal, and occipital lobes (Fischl et al. 2004; Desikan et al. 2006).

For quantitative sulcal pattern analysis, global patterning of primary sulci was represented with a graph structure using sulcal pits and their surrounding catchment basins (Im, et al. 2011b). Sulcal pits are the deepest local points in catchment basins of primary sulci (Lohmann and von Cramon 2000; Im et al. 2010) and their spatial distribution has been observed to be temporally stable against dynamic brain growth and related to brain functions under genetic control in our prior studies (Im, et al. 2011a; Im and Grant 2019). We generated a sulcal depth map on the inner cortical surface using Freesurfer and smoothed the map using a surface-based heat kernel smoothing with a full-width half-maximum of 10 mm (Chung et al. 2005; Im et al. 2010). Sulcal pits and their basins were automatically identified using a watershed-based image-processing algorithm using the smoothed depth map of the inner cortical surface. Sulcal pits were used as the nodes in the graph representation of sulcal pattern and when sulcal catchment basins met, sulcal pits in those basins were connected with an edge. The sulcal graph structure includes geometric features of nodes (3D position [x, y, z], area [s], and depth [d] of sulcal pits and basins); their intersulcal geometric relationships; and graph topology (the number of edges and the paths between nodes [c]) to characterize the interrelated sulcal arrangement and patterning. These features were weighted to give their relative importance, $F = (w_x x, w_y y, w_z z, w_s s, w_d d, w_c c)$. We determined the optimal match of sulcal pits having the minimum difference of the features between 2 sulcal graphs by using a spectral matching technique (Im, et al. 2011b) (Fig. 1). We then computed their similarity using an exponential function based on the difference of 2 sulcal feature sets, which ranged from 0 to 1. All features were optimally weighted for the sulcal pattern similarity to have mean and standard deviation (SD) values of about ~0.75 and 0.01–0.03 respectively. After measuring the similarity with all combined features (sulcal position, area, depth, and graph topology), we further measured the similarity using each individual feature by setting all of the weights of the other features to 0 to evaluate their relative importance on the composite similarity. Using this graph-based sulcal pattern comparison method, we examined intergenerational transmission of sulcal patterns by testing

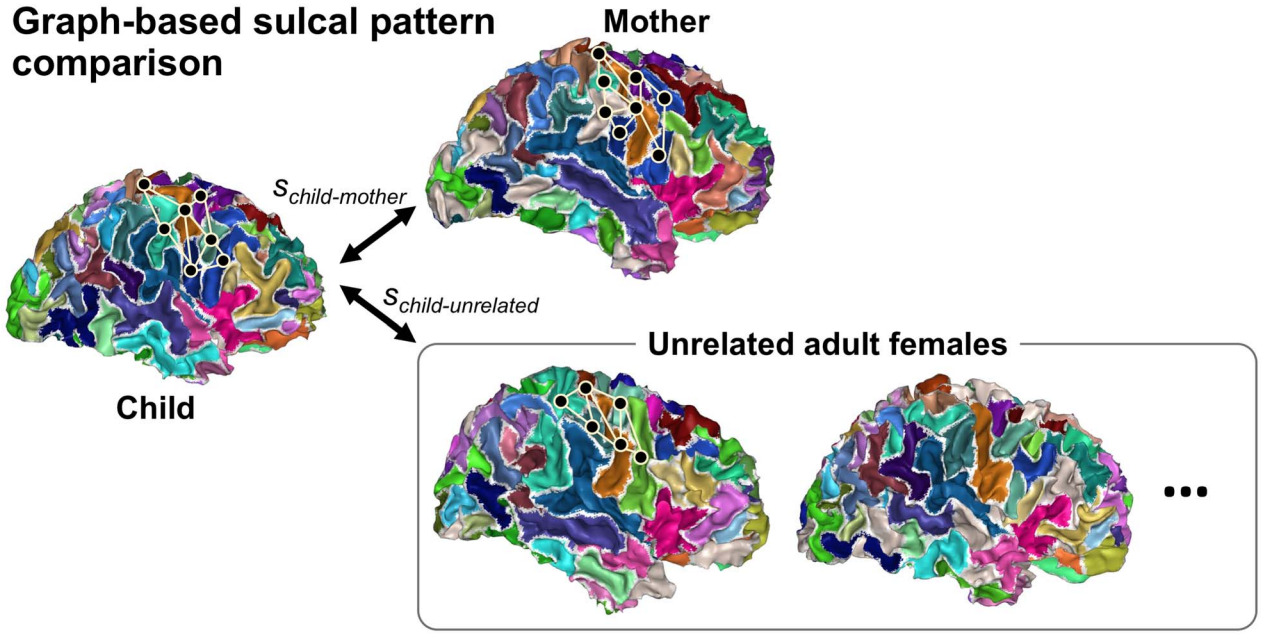

Figure 1. Sulcal pits (black spheres) and their corresponding sulcal basins (colored patches) are automatically extracted on the white matter surface using the watershed segmentation applied to sulcal depth map. Each sulcal pit corresponds to a node in the graph structure. When sulcal basins meet, sulcal pits in those basins are connected with an undirected edge. Two sulcal graphs are optimally matched and their similarity is measured by using the geometric features of nodes (3D position, depth and area of sulcal basin) and their relationship between the nodes, and the graph topological features (the number of edges and the paths between nodes). The sulcal basins paired by matching are marked with the same color. Sulcal pattern similarities were measured between children and their mothers and between children and unrelated adult females.

whether the sulcal pattern similarities between all children and their mothers were significantly different when compared to the similarities between all children and unrelated adults. We then compared the intergenerational transmission of sulcal patterns between daughter–mother versus son–mother pairs. For each child, the sulcal pattern similarity with his/her mother ($S_{child-mother}$) as well as the mean similarity with the other 14 adult females ($S_{child\text{-}unrelated}$) were computed (Figs 1 and 2). Our method for sulcal pit extraction and pattern analysis has been validated, showing high reliability across different sites, scanners, and magnet strengths (Im, et al. 2013a; Morton et al. 2019), and applied to our many previous studies (Im, et al. 2013b; Im et al. 2016; Im and Grant 2019; Morton et al. 2019).

Statistical Analysis

For the child–mother (or son–mother and daughter–mother) pairs, the similarity value between 1 child and his/her mother is calculated. For the child-unrelated (or son-unrelated and daughter-unrelated) pairs, each child is paired with each adult who is not his/her mother and an average similarity value is calculated to be included in the analyses.

First, we measured the difference in the sulcal pattern similarity between child–mother and child-unrelated pairs (Fig. 2). For this, we have defined the following index indicating intergenerational transmission of sulcal patterns (S_{InterG}).

$$S_{InterG} = S_{child-mother} - S_{child-unrelated}$$

Then, we statistically tested if the mean of S_{InterG} distribution was different from 0 using a one-sample *t*-test for different feature sets (sulcal position, area, depth, graph topology, and the combined features) in the left and right frontal, parietal, temporal, and occipital lobes.

Second, the difference in sulcal pattern similarity between son–mother and son-unrelated pairs ($S_{InterG.s}$) was statistically compared with the difference in sulcal pattern similarity between daughter–mother and daughter-unrelated pairs ($S_{InterG.d}$) using an independent two samples *t*-test in the left and right frontal, parietal, temporal, and occipital lobes.

$$S_{InterG.s} = S_{son-mother} - S_{son-unrelated}$$

$$S_{InterG.d} = S_{daughter-mother} - S_{daughter-unrelated}$$

False discovery rate (FDR) control method at a *q*-value (FDR adjusted/corrected *P* value) of 0.05 was used to adjust for multiple group comparisons within each hemisphere (Benjamini and Hochberg 1995; Genovese et al. 2002).

Results

Sulcal Pattern Similarity between Child–Mother and Child-Unrelated Pairs:

Statistical comparisons of the sulcal pattern similarity between the child–mother ($N = 16$) and between child-unrelated ($N = 16$) groups for different feature sets are reported in Table 2. After FDR correction for multiple comparisons, in the right hemisphere, right frontal lobe depth ($P = 0.0001$) and area ($P = 0.004$), and right parietal lobe graph ($P = 0.006$) sulcal pattern features remained significantly higher in the child–mother pairs compared to child-unrelated pairs (Supplementary Fig. S1). These

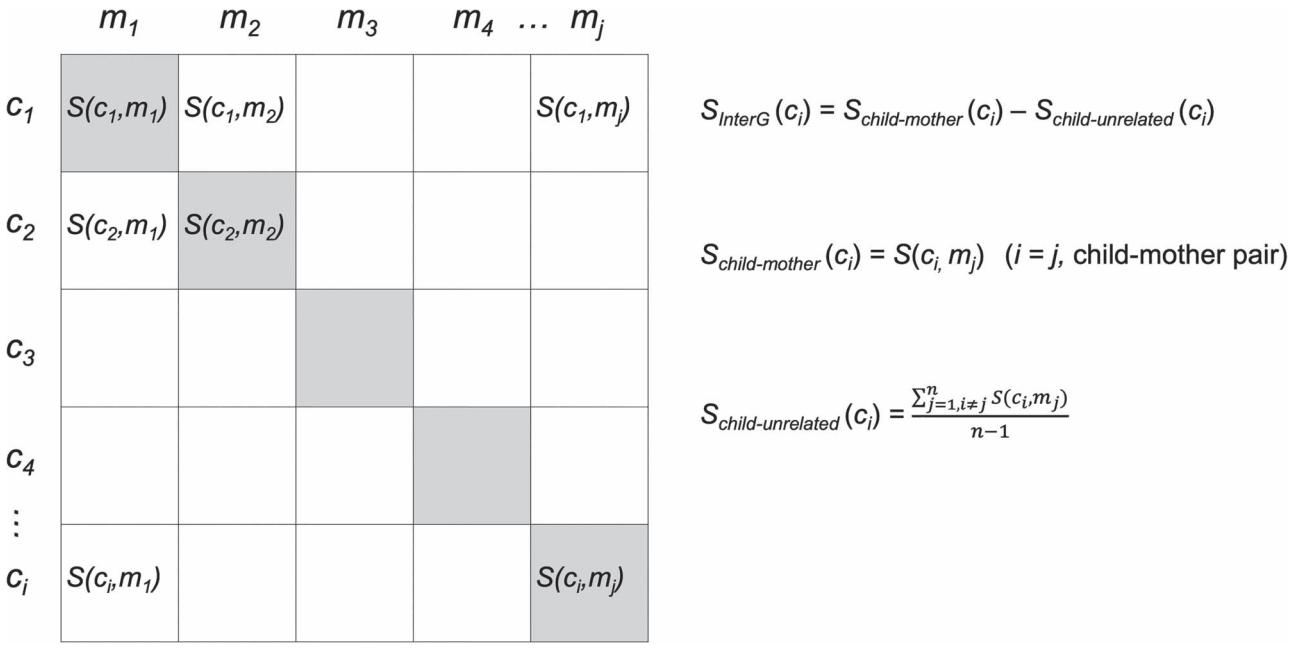

Figure 2. Sulcal pattern similarity matrix depicting child–mother (gray squares) and child-unrelated (white squares) pairs. S_{InterG} is defined as the difference in the sulcal pattern similarity between child–mother and child-unrelated pairs. $S_{child-mother}$ is defined as the sulcal pattern similarity between child–mother pairs and $S_{child-unrelated}$ is defined as the mean sulcal pattern similarity between child-unrelated pairs. c_i is a child participant, m_j is a mother participant, S is the sulcal pattern similarity between a child and a mother participant, and n is the number of mothers.

results remained significant once we redid the analysis after removing one of the child–mother pairs from the analysis, where the mother is identical. After FDR correction for multiple comparisons, there were no significant results for the left hemisphere for the sulcal pattern similarity between child–mother and child-unrelated pairs.

When FDR correction was not applied, in the left hemisphere, the results showed that sulcal pattern similarity was significantly higher in child–mother pairs, compared to the child-unrelated pairs, in the left temporal lobe for the total sulcal pattern feature ($P = 0.032$). There were no other significant differences between the child–mother pairs and the child-unrelated pairs in the other left hemisphere lobes or their associated sulcal pattern features ($p > 0.05$). Without FDR correction, in the right hemisphere, sulcal pattern similarity was higher for child–mother pairs than child-unrelated pairs in the right frontal lobe for total ($P = 0.031$), position ($P = 0.021$), depth ($P = 0.0001$), and area ($P = 0.004$) sulcal pattern features; in the right parietal lobe for total ($P = 0.027$), and graph ($P = 0.006$) sulcal pattern features; and in the right occipital lobe for the total sulcal pattern feature ($P = 0.015$). There were no significant differences for any of the sulcal pattern features in the right temporal lobe.

Sulcal Pattern Similarity between Son–Mother and Son-Unrelated as well as Daughter–Mother and Daughter-Unrelated Pairs

Statistical comparisons of the sulcal pattern similarity between son–mother and son-unrelated pairs ($S_{InterG.s}$) as well as the difference in sulcal pattern similarity between daughter–mother and daughter-unrelated pairs ($S_{InterG.d}$) for different feature sets are reported in Table 3. There were no significant results after FDR correction for multiple comparisons.

The following results were obtained without FDR correction. $S_{InterG.s}$ was greater than $S_{InterG.d}$ in the left frontal lobe for area sulcal pattern feature ($P = 0.031$). In the left temporal lobe, $S_{InterG.s}$ was greater than $S_{InterG.d}$ for total ($P = 0.026$) and $S_{InterG.d}$ was greater than $S_{InterG.s}$ for graph ($P = 0.025$) sulcal pattern features. $S_{InterG.d}$ was greater than $S_{InterG.s}$ in the left parietal lobe for depth sulcal pattern feature ($P = 0.029$). In the left occipital lobe, $S_{InterG.d}$ was greater than $S_{InterG.s}$ for both position ($P = 0.021$) and area ($P = 0.009$) sulcal pattern features. In the right frontal lobe $S_{InterG.s}$ was greater than $S_{InterG.d}$ for area sulcal pattern feature ($P = 0.025$). $S_{InterG.s}$ was greater than $S_{InterG.d}$ in the right parietal lobe for position sulcal pattern feature ($P = 0.044$). There were no other significant differences in the other lobes of the right hemisphere.

Discussion

This is the first study to examine the intergenerational transmission of cortical sulcal patterns. As hypothesized, we have shown stronger sulcal pattern similarity for child–mother pairs than child-unrelated pairs. Our graph-based sulcal pattern comparison method detected higher similarity between child–mother pairs mostly for the right lobar regions. We have also shown that child–mother versus child-unrelated pairs differed for daughters and sons; however, none of these differences survived multiple comparison corrections.

Intergenerational transmission of neuronal structure has been shown in previous studies. For example, the regional gray matter volume in corticolimbic circuitry (Yamagata et al. 2016) and cortical gray matter thickness (Foland-Ross et al. 2016) showed a stronger matrilineal transmission pattern. Volumetric measurements such as gray matter volume and cortical thickness are affected largely by the developmental changes

Table 2 Statistical comparisons of the sulcal pattern similarity between the child–mother ($N = 16$) and between child-unrelated ($N = 16$) groups for different feature sets. Data are presented as mean (SD), $*P < 0.05$, $**$FDR $q < 0.05$

Location	Sulcal pattern feature	Child–mother Mean (std)	Child-unrelated Mean (std)	*P* value
LH	Total	0.7527 (0.0104)	0.7495 (0.0083)	0.1678
	Position	0.7993 (0.0132)	0.7943 (0.0086)	0.0789
	Depth	0.8185 (0.0169)	0.8153 (0.0086)	0.4242
	Area	0.8900 (0.0086)	0.8897 (0.0044)	0.8696
	Graph	0.8844 (0.0147)	0.8855 (0.0105)	0.7809
LF	Total	0.7596 (0.0124)	0.7614 (0.0078)	0.5478
	Position	0.8008 (0.0167)	0.8038 (0.0076)	0.4766
	Depth	0.8144 (0.0225)	0.8201 (0.0083)	0.2242
	Area	0.8945 (0.0201)	0.8957 (0.0065)	0.7634
	Graph	0.9013 (0.0125)	0.8977 (0.0105)	0.3656
LT	Total	0.7670 (0.0294)	0.7507 (0.0213)	0.032*
	Position	0.8084 (0.0402)	0.7968 (0.0194)	0.2901
	Depth	0.8205 (0.0227)	0.8092 (0.0175)	0.1273
	Area	0.8856 (0.0272)	0.8741 (0.0179)	0.1046
	Graph	0.9099 (0.0199)	0.9033 (0.0143)	0.1857
LP	Total	0.7354 (0.0212)	0.7288 (0.0175)	0.2624
	Position	0.8145 (0.0289)	0.8049 (0.0091)	0.2095
	Depth	0.7982 (0.0354)	0.7911 (0.0141)	0.4251
	Area	0.8593 (0.0250)	0.8570 (0.0162)	0.7158
	Graph	0.8691 (0.0327)	0.8729 (0.0266)	0.6453
LO	Total	0.7301 (0.0375)	0.7305 (0.0161)	0.971
	Position	0.8000 (0.0281)	0.8032 (0.0167)	0.7381
	Depth	0.8005 (0.0379)	0.7960 (0.0174)	0.699
	Area	0.8752 (0.0339)	0.8764 (0.0206)	0.8467
	Graph	0.8701 (0.0511)	0.8688 (0.0219)	0.917
RH	Total	0.7588 (0.0165)	0.7494 (0.0071)	0.0185*
	Position	0.8017 (0.0152)	0.7945 (0.0064)	0.0345*
	Depth	0.8220 (0.0160)	0.8178 (0.0085)	0.2959
	Area	0.8928 (0.0122)	0.8878 (0.0059)	0.1036
	Graph	0.8895 (0.0173)	0.8845 (0.0134)	0.0799
RF	Total	0.7744 (0.0176)	0.7648 (0.0096)	0.031*
	Position	0.8097 (0.0179)	0.7983 (0.0093)	0.0205*
	Depth	0.8329 (0.0110)	0.8228 (0.0094)	0.0001**
	Area	0.9061 (0.0150)	0.8977 (0.0087)	0.0044**
	Graph	0.9036 (0.0175)	0.9067 (0.0084)	0.4621
RT	Total	0.7570 (0.0339)	0.7518 (0.0162)	0.5498
	Position	0.8218 (0.0313)	0.8089 (0.0146)	0.1248
	Depth	0.8243 (0.0303)	0.8249 (0.0152)	0.9462
	Area	0.8700 (0.0334)	0.8693 (0.0132)	0.9455
	Graph	0.8855 (0.0358)	0.8897 (0.0274)	0.601
RP	Total	0.7298 (0.0300)	0.7183 (0.0217)	0.0265*
	Position	0.8041 (0.0220)	0.8011 (0.0107)	0.5587
	Depth	0.7857 (0.0305)	0.7866 (0.0182)	0.8628
	Area	0.8533 (0.0333)	0.8465 (0.0273)	0.2452
	Graph	0.8826 (0.0294)	0.8670 (0.0184)	0.0064**
RO	Total	0.7488 (0.0235)	0.7344 (0.0127)	0.0152*
	Position	0.8063 (0.0351)	0.7985 (0.0096)	0.4002
	Depth	0.8102 (0.0392)	0.8000 (0.0143)	0.3273
	Area	0.8816 (0.0245)	0.8751 (0.0128)	0.3434
	Graph	0.8853 (0.0439)	0.8757 (0.0238)	0.4518

that occur postnatally over the years through adulthood (Shaw et al. 2008). The primary cortical sulcal pattern characterized in the present and previous studies, namely the global patterns of arrangement, number, and size of sulcal folds, is noticeable in the fetal brain before the third trimester, during the radial growth stage of the cerebral cortex (Foland-Ross et al. 2016), and are fully determined before birth (Im and Grant 2019). Early cortical folds are thought to develop into the deepest points of the primary sulci (Im et al. 2010), they are strongly under genetic control and go through little change postnatally (Garel et al. 2001; Rakic 2004; Kostovic and Vasung 2009; Hill et al. 2010; Meng et al. 2014; Rash and Rakic 2014; Sun and Hevner 2014; de Juan Romero et al. 2015; Cachia et al. 2016; Le Guen, et al. 2018a). Heritability of cortical folding has also been shown for specific brain regions related to certain cognitive functions such as language (Le Guen, et al. 2018b), and for

Table 3 Statistical comparisons of the sulcal pattern similarity between son–mother and son-unrelated pairs ($S_{InterG.s}$) with the difference in sulcal pattern similarity between daughter–mother and daughter-unrelated pairs ($S_{InterG.d}$) for different feature sets. Data are presented as mean (SD), $*P < 0.05$, $**$FDR $q < 0.05$

Location	Sulcal pattern feature	Son (pair-unrelated) Mean (std)	Daughter (pair-unrelated) Mean (std)	*P* value
LH	Total	0.0032 (0.0101)	0.0030 (0.0076)	0.9645
	Position	0.0083 (0.0131)	0.0018 (0.0072)	0.242
	Depth	0.0022 (0.0143)	0.0044 (0.0184)	0.7949
	Area	0.0004 (0.0098)	0.0002 (0.0066)	0.9661
	Graph	−0.0035 (0.0158)	0.0014 (0.0143)	0.5241
LF	Total	−0.0020 (0.0166)	−0.0016 (0.0050)	0.9509
	Position	−0.0038 (0.0213)	−0.0022 (0.0110)	0.8572
	Depth	−0.0031 (0.0127)	−0.0084 (0.0229)	0.5771
	Area	0.0069 (0.0106)	−0.0093 (0.0159)	0.0308*
	Graph	−0.0007 (0.0118)	0.0080 (0.0185)	0.2761
LT	Total	0.0015 (0.0157)	0.0310 (0.0295)	0.0257*
	Position	−0.0030 (0.0291)	0.0262 (0.0499)	0.1743
	Depth	0.0055 (0.0225)	0.0170 (0.0330)	0.4297
	Area	0.0075 (0.0247)	0.0155 (0.0295)	0.5629
	Graph	−0.0036 (0.0189)	0.0168 (0.0132)	0.025*
LP	Total	−0.0008 (0.0239)	0.0139 (0.0197)	0.2034
	Position	0.0009 (0.0271)	0.0183 (0.0305)	0.246
	Depth	−0.0112 (0.0365)	0.0254 (0.0217)	0.0289*
	Area	−0.0090 (0.0238)	0.0136 (0.0208)	0.0632
	Graph	0.0059 (0.0319)	−0.0135 (0.0318)	0.2413
LO	Total	−0.0041 (0.0267)	0.0035 (0.0395)	0.6589
	Position	−0.0238 (0.0356)	0.0174 (0.0272)	0.0209*
	Depth	−0.0069 (0.0242)	0.0159 (0.0599)	0.3361
	Area	−0.0172 (0.0179)	0.0146 (0.0234)	0.0087*
	Graph	0.0246 (0.0409)	−0.0220 (0.0466)	0.0513
RH	Total	0.0116 (0.0161)	0.0072 (0.0128)	0.5487
	Position	0.0074 (0.0113)	0.0068 (0.0139)	0.9219
	Depth	0.0037 (0.0176)	0.0047 (0.0140)	0.9018
	Area	0.0095 (0.0114)	0.0005 (0.0105)	0.1265
	Graph	0.0068 (0.0123)	0.0031 (0.0087)	0.4947
RF	Total	0.0094 (0.0198)	0.0097 (0.0127)	0.9724
	Position	0.0097 (0.0221)	0.0131 (0.0130)	0.7112
	Depth	0.0076 (0.0061)	0.0125 (0.0092)	0.2308
	Area	0.0138 (0.0098)	0.0030 (0.0072)	0.0245*
	Graph	−0.0021 (0.0185)	−0.0041 (0.0151)	0.821
RT	Total	0.0020 (0.0305)	0.0084 (0.0391)	0.7222
	Position	0.0137 (0.0198)	0.0121 (0.0419)	0.9233
	Depth	0.0029 (0.0395)	−0.0041 (0.0322)	0.6996
	Area	−0.0018 (0.0399)	0.0030 (0.0344)	0.8005
	Graph	−0.0105 (0.0309)	0.0020 (0.0336)	0.4509
RP	Total	0.0141 (0.0223)	0.0089 (0.0155)	0.5947
	Position	0.0129 (0.0184)	−0.0069 (0.0174)	0.0437*
	Depth	−0.0003 (0.0180)	−0.0014 (0.0228)	0.9139
	Area	0.0054 (0.0254)	0.0083 (0.0210)	0.8048
	Graph	0.0120 (0.0244)	0.0193 (0.0146)	0.4796
RO	Total	0.0078 (0.0249)	0.0210 (0.0150)	0.2217
	Position	0.0022 (0.0379)	0.0133 (0.0353)	0.5569
	Depth	−0.0003 (0.0368)	0.0207 (0.0435)	0.3133
	Area	0.0086 (0.0344)	0.0043 (0.0173)	0.7606
	Graph	0.0080 (0.0550)	0.0113 (0.0477)	0.8992

aging and cognitive decline (Le Guen et al. 2019); therefore, they may be a more reliable measure for intergenerational transmission of neuronal structure, starting even in the prenatal period. Our finding of significant similarity between children and their mothers compared to the similarity between children and unrelated female adults supports the genetic influence on sulcal patterning. Our results are consistent with the findings of previous twin studies that reported significant genetic effects on the sulcal patterns and pits (Im, et al. 2011b; Le Guen, et al. 2018a).

Among sulcal pattern features examined, our results showed that depth, area, and graph topological sulcal pattern features were significantly higher in the child–mother pairs. Based on the protomap hypothesis, cortical neurons originated in the

proliferative zones (ventricular zone [VZ] and subventricular zone [SVZ]) carry intrinsic programs for cortical functional arealization and migrate to their proper laminar and areal positions during fetal development (Rakic 1988, 2009). Optimal organization and arrangement of cortical functional areas predetermined from the genetic protomap of VZ may give rise to specific topological and areal pattern of sulcal folds in the human brain (Klyachko and Stevens 2003; Rakic 2004; O'Leary et al. 2007; Fischl et al. 2008; Im et al. 2010; Im, et al. 2011a; Sun and Hevner 2014). Moreover, cortical surface expansion and deep sulcal folding occur through the proliferation and expansion of neural stem cells and progenitors in the VZ and SVZ (Chenn and Walsh 2002; Rakic 2009; Lui et al. 2011; Sun and Hevner 2014). Thus, we hypothesize that the genetic protomap of VZ and the amount and spatial pattern of neural proliferation in the proliferative zones may be highly heritable, and this may result in high similarity of depth, area, and graph topological sulcal patterns in the child–mother pairs but not in unrelated pairs.

The significant similarity between children and their mothers was more pronounced in the right hemisphere, which is consistent with the existing findings that right hemisphere showed heritability for sulcal width (Pizzagalli et al. 2020) and that the right hemisphere is more affected by genetic factors than the left hemisphere (Geschwind et al. 2002; Dubois et al. 2008). Frontal regions of the brain encompass a functional network responsible for executive function (DeRight 2019), emotional expression (Dixon et al. 2017), problem solving (Luria and Tsvetkova 1990), attention (Bahmani et al. 2019), and working memory (Bahmani et al. 2019). High similarity between child–mother pairs for the right frontal lobar regions might indicate that such functions can have heritable characteristics. Atypical frontal lobe function such as executive function and working memory impairments and atypical emotional expressions are seen in disorders such as attention deficit hyperactivity disorder and autism spectrum disorders (Pugliese et al. 2015; Kofler et al. 2018; Rabiee et al. 2018; Grabowski et al. 2019; Otterman et al. 2019; Sánchez et al. 2019). It is possible that our results can shed light into the intergenerational transmission of brain structure in these and other highly hereditary disorders. Parietal lobes have been shown to be associated with a functional network responsible for episodic (Berryhill et al. 2010) and working (Cabeza et al. 2008) memory, conceptual processing of numbers (Cappelletti et al. 2010), judgment of temporal order of events (Battelli et al. 2007), and distinguishing one's own actions from those of others that have been shown to be functioning abnormally in patients with schizophrenia (Kato et al. 2011). High similarity for child–mother pairs for the right parietal lobe might suggest increased heritability for these brain functions and associated disorders. Previous studies that examined genetic influence of sulcal patterns and pits in twins found more similarity in twin pairs compared to unrelated pairs in the sulcal patterns in many regions in the brain, of both hemispheres and all lobar regions (Im, et al. 2011b), and in the central, cingulate, collateral, occipitotemporal, parieto-occipital, and superior temporal sulci (Le Guen, et al. 2018a). Whereas in our study, the significant results pointed to fewer regions than those reported in twin studies. These differences could be explained by the fewer common genes being shared between a mother and her child compared to the common genes shared between twin pairs.

One major limitation of this study is that we did not examine data from fathers or adult unrelated males. To understand the full picture of intergenerational transmission of sulcal patterns, and how sulcal patterns in different regions of the brain are selectively transmitted from mothers and fathers to their daughters and sons, a future study that also includes data from fathers as well as unrelated males would be necessary. This would also help understand how much of the intergenerational transmission is due to pure genetics versus being exposed to certain factors in utero such as stressors or nutrients during pregnancy. Furthermore, we did not assess mothers for factors that have been shown to affect prenatal brain development, such as childhood maltreatment exposure (Moog et al. 2018). We were also not able to assess the genetic and environmental effects separately since we did not have children who were adopted by the same mothers and raised in the same environment as the biological children of these mothers. We also did not have biological children who lived with other mothers in different environments. We also did not have any household environment information on the participants in our study. Another limitation of our study was the sample size, especially in the son-mother and daughter-mother pairs. A larger sample size could have helped detect smaller effects and help delineate better the difference between sons and daughters.

Conclusion

This is the first study to analyze intergenerational transmission of brain sulcal patterns. We have observed increased sulcal pattern similarity between children and their mothers compared to children and unrelated female adults. Future studies with larger sample sizes that include fathers and unrelated male adults would be helpful to further understand the selective role of mothers versus fathers in the intergenerational transmission of sulcal patterns as well as the role of genetic influences versus other factors the fetus is exposed to in the intrauterine environment during the prenatal period.

Supplementary Material

Supplementary material can be found at *Cerebral Cortex* online.

Notes

We would like to thank the families who participated in this study. We are also thankful to the staff at Boston Children's Hospital who facilitated data collection; Jade Dunstan, Clarisa Carruthers, Doroteja Rubez, Minju (Ally) Lee, Kathryn Garrisi; and to the staff at A.A. Martinos Center for Biomedical Imaging who helped with data preprocessing: Emma Boyd and Holly Freeman. *Conflict of interest:* None declared.

Funding

Eunice Kennedy Shriver National Institute of Child Health & Human Development of the National Institutes of Health (NIH) (R01 HD065762), the William Hearst Fund (Harvard University), and the Harvard Catalyst/NIH (5UL1RR025758) to N.G. and P.E.G.

References

Aktar E, Nikolić M, Bögels SM. 2017. Environmental transmission of generalized anxiety disorder from parents to children: worries, experiential avoidance, and intolerance of uncertainty. *Dialogues Clin Neurosci*. 19:137–147.

Bahmani Z, Clark K, Merrikhi Y, Mueller A, Pettine W, Isabel Vanegas M, Moore T, Noudoost B. 2019. Prefrontal contributions to attention and working memory. *Curr Top Behav Neurosci*. 41:129–153.

Battelli L, Pascual-Leone A, Cavanagh P. 2007. The "when" pathway of the right parietal lobe. *Trends Cogn Sci*. 11: 204–210.

Benjamini Y, Hochberg Y. 1995. Controlling the false discovery rate: a practical and powerful approach to multiple testing. *J R Stat Soc B Methodol*. 57:289–300.

Berryhill ME, Wencil EB, Branch Coslett H, Olson IR. 2010. A selective working memory impairment after transcranial direct current stimulation to the right parietal lobe. *Neurosci Lett*. 479:312–316.

Cabeza R, Ciaramelli E, Olson IR, Moscovitch M. 2008. The parietal cortex and episodic memory: an attentional account. *Nat Rev Neurosci*. 9:613–625.

Cachia A, Borst G, Tissier C, Fisher C, Plaze M, Gay O, Rivière D, Gogtay N, Giedd J, Mangin J-F *et al*. 2016. Longitudinal stability of the folding pattern of the anterior cingulate cortex during development. *Dev Cogn Neurosci*. 19:122–127.

Cappelletti M, Lee HL, Freeman ED, Price CJ. 2010. The role of right and left parietal lobes in the conceptual processing of numbers. *J Cogn Neurosci*. 22:331–346.

Chenn A, Walsh CA. 2002. Regulation of cerebral cortical size by control of cell cycle exit in neural precursors. *Science*. 297:365–369.

Chung MK, Robbins SM, Dalton KM, Davidson RJ, Alexander AL, Evans AC. 2005. Cortical thickness analysis in autism with heat kernel smoothing. *Neuroimage*. 25:1256–1265.

Curley JP, Mashoodh R. 2010. Parent-of-origin and transgenerational germline influences on behavioral development: the interacting roles of mothers, fathers, and grandparents. *Dev Psychobiol*. 52:312–330.

de Juan Romero C, Bruder C, Tomasello U, Sanz-Anquela JM, Borrell V. 2015. Discrete domains of gene expression in germinal layers distinguish the development of gyrencephaly. *EMBO J*. 34:1859–1874.

DeRight J. 2019. History of "frontal" syndromes and executive dysfunction. *Front Neurol Neurosci*. 44:100–107.

Desikan RS, Ségonne F, Fischl B, Quinn BT, Dickerson BC, Blacker D, Buckner RL, Dale AM, Maguire RP, Hyman BT *et al*. 2006. An automated labeling system for subdividing the human cerebral cortex on MRI scans into gyral based regions of interest. *Neuroimage*. 31:968–980.

Dixon ML, Thiruchselvam R, Todd R, Christoff K. 2017. Emotion and the prefrontal cortex: an integrative review. *Psychol Bull*. 143:1033–1081.

D'Onofrio BM, Slutske WS, Turkheimer E, Emery RE, Paige Harden K, Heath AC, Madden PAF, Martin NG. 2007. Intergenerational transmission of childhood conduct problems. *Arch Gen Psychiatry*. 64:820–829.

Dubois J, Benders M, Cachia A, Lazeyras F, Ha-Vinh Leuchter R, Sizonenko SV, Borradori-Tolsa C, Mangin JF, Hüppi PS. 2008. Mapping the early cortical folding process in the preterm newborn brain. *Cereb Cortex*. 18:1444–1454.

Fischl B. 2012. FreeSurfer. *Neuroimage*. 62:774–781.

Fischl B, Rajendran N, Busa E, Augustinack J, Hinds O, Yeo BTT, Mohlberg H, Amunts K, Zilles K. 2008. Cortical folding patterns and predicting cytoarchitecture. *Cereb Cortex*. 18:1973–1980.

Fischl B, van der Kouwe A, Destrieux C, Halgren E, Ségonne F, Salat DH, Busa E, Seidman LJ, Goldstein J, Kennedy D *et al*. 2004. Automatically parcellating the human cerebral cortex. *Cereb Cortex*. 14:11–22.

Flint J, Timpson N, Munafò M. 2014. Assessing the utility of intermediate phenotypes for genetic mapping of psychiatric disease. *Trends Neurosci*. 37:733–741.

Foland-Ross LC, Behzadian N, LeMoult J, Gotlib IH. 2016. Concordant patterns of brain structure in mothers with recurrent depression and their never-depressed daughters. *Dev Neurosci*. 38:115–123.

Garel C, Chantrel E, Brisse H, Elmaleh M, Luton D, Oury JF, Sebag G, Hassan M. 2001. Fetal cerebral cortex: normal gestational landmarks identified using prenatal MR imaging. *AJNR Am J Neuroradiol*. 22:184–189.

Garel C, Chantrel E, Elmaleh M, Brisse H, Sebag G. 2003. Fetal MRI: normal gestational landmarks for cerebral biometry, gyration and myelination. *Childs Nerv Syst*. 19:422–425.

Genovese CR, Lazar NA, Nichols T. 2002. Thresholding of statistical maps in functional neuroimaging using the false discovery rate. *Neuroimage*. 15:870–878.

Geschwind DH, Miller BL, DeCarli C, Carmelli D. 2002. Heritability of lobar brain volumes in twins supports genetic models of cerebral laterality and handedness. *Proc Natl Acad Sci*. 99:3176–3181.

Grabowski K, Rynkiewicz A, Lassalle A, Baron-Cohen S, Schuller B, Cummins N, Baird A, Podgórska-Bednarz J, Pieniążek A, Łucka I. 2019. Emotional expression in psychiatric conditions: new technology for clinicians. *Psychiatry Clin Neurosci*. 73:50–62.

Hill J, Inder T, Neil J, Dierker D, Harwell J, Van Essen D. 2010. Similar patterns of cortical expansion during human development and evolution. *Proc Natl Acad Sci USA*. 107:13135–13140.

Ho TC, Sanders SJ, Gotlib IH, Hoeft F. 2016. Intergenerational neuroimaging of human brain circuitry. *Trends Neurosci*. 39:644–648.

Im K, Choi YY, Yang J-J, Lee KH, Kim SI, Grant PE, Lee J-M. 2011a. The relationship between the presence of sulcal pits and intelligence in human brains. *Neuroimage*. 55:1490–1496.

Im K, Grant PE. 2019. Sulcal pits and patterns in developing human brains. *Neuroimage*. 185:881–890.

Im K, Jo HJ, Mangin J-F, Evans AC, Kim SI, Lee J-M. 2010. Spatial distribution of deep sulcal landmarks and hemispherical asymmetry on the cortical surface. *Cereb Cortex*. 20:602–611.

Im K, Lee J-M, Jeon S, Kim J-H, Seo SW, Na DL, Grant PE. 2013a. Reliable identification of deep sulcal pits: the effects of scan session, scanner, and surface extraction tool. *PLoS One*. 8:e53678.

Im K, Pienaar R, Lee J-M, Seong J-K, Choi YY, Lee KH, Grant PE. 2011b. Quantitative comparison and analysis of sulcal patterns using sulcal graph matching: a twin study. *Neuroimage*. 57:1077–1086.

Im K, Pienaar R, Paldino MJ, Gaab N, Galaburda AM, Grant PE. 2013b. Quantification and discrimination of abnormal sulcal patterns in polymicrogyria. *Cereb Cortex*. 23: 3007–3015.

Im K, Raschle NM, Smith SA, Ellen Grant P, Gaab N. 2016. Atypical Sulcal pattern in children with developmental dyslexia and at-risk kindergarteners. *Cereb Cortex*. 26:1138–1148.

Kato Y, Muramatsu T, Kato M, Shibukawa Y, Shintani M, Mimura M. 2011. Magnetoencephalography study of right parietal lobe dysfunction of the evoked mirror neuron system in antipsychotic-free schizophrenia. *PLoS One*. 6:e28087.

Klapwijk ET, van de Kamp F, van der Meulen M, Peters S, Wierenga LM. 2019. Qoala-T: a supervised-learning tool for

quality control of FreeSurfer segmented MRI data. *Neuroimage*. 189:116–129.

Klyachko VA, Stevens CF. 2003. Connectivity optimization and the positioning of cortical areas. *Proc Natl Acad Sci U S A*. 100:7937–7941.

Kochunov P, Castro C, Davis D, Dudley D, Brewer J, Zhang Y, Kroenke CD, Purdy D, Fox PT, Simerly C *et al*. 2010. Mapping primary gyrogenesis during fetal development in primate brains: high-resolution in utero structural MRI of fetal brain development in pregnant baboons. *Front Neurosci*. 4:20.

Kofler MJ, Sarver DE, Harmon SL, Moltisanti A, Aduen PA, Soto EF, Ferretti N. 2018. Working memory and organizational skills problems in ADHD. *J Child Psychol Psychiatry*. 59:57–67.

Kostovic I, Vasung L. 2009. Insights from in vitro fetal magnetic resonance imaging of cerebral development. *Semin Perinatol*. 33:220–233.

Le Guen Y, Auzias G, Leroy F, Noulhiane M, Dehaene-Lambertz G, Duchesnay E, Mangin J-F, Coulon O, Frouin V. 2018a. Genetic influence on the Sulcal pits: on the origin of the first cortical folds. *Cereb Cortex*. 28:1922–1933.

Le Guen Y, Leroy F, Auzias G, Riviere D, Grigis A, Mangin J-F, Coulon O, Dehaene-Lambertz G, Frouin V. 2018b. The chaotic morphology of the left superior temporal sulcus is genetically constrained. *Neuroimage*. 174:297–307.

Le Guen Y, Philippe C, Riviere D, Lemaitre H, Grigis A, Fischer C, Dehaene-Lambertz G, Mangin J-F, Frouin V. 2019. eQTL of KCNK2 regionally influences the brain sulcal widening: evidence from 15,597 UK biobank participants with neuroimaging data. *Brain Struct Funct*. 224:847–857.

Lohmann G, von Cramon DY. 2000. Automatic labelling of the human cortical surface using sulcal basins. *Med Image Anal*. 4:179–188.

Lui JH, Hansen DV, Kriegstein AR. 2011. Development and evolution of the human neocortex. *Cell*. 146:18–36.

Luria AR, Tsvetkova LS. 1990. Disorders of problem solving with secondary frontal syndrome. In: *The neuropsychological analysis of problem solving*. 1st ed. CRC Press. p. 161–173.

Meng Y, Li G, Lin W, Gilmore JH, Shen D. 2014. Spatial distribution and longitudinal development of deep cortical sulcal landmarks in infants. *Neuroimage*. 100:206–218.

Moog NK, Entringer S, Rasmussen JM, Styner M, Gilmore JH, Kathmann N, Heim CM, Wadhwa PD, Buss C. 2018. Intergenerational effect of maternal exposure to childhood maltreatment on Newborn brain anatomy. *Biol Psychiatry*. 83:120–127.

Morton SU, Maleyeff L, Wypij D, Yun HJ, Newburger JW, Bellinger DC, Roberts AE, Rivkin MJ, Seidman JG, Seidman CE *et al*. 2019. Abnormal left-hemispheric Sulcal patterns correlate with neurodevelopmental outcomes in subjects with single ventricular congenital heart disease. *Cereb Cortex*. 30:476–487.

O'Leary DDM, Chou S-J, Sahara S. 2007. Area patterning of the mammalian cortex. *Neuron*. 56:252–269.

Otterman DL, Koopman-Verhoeff ME, White TJ, Tiemeier H, Bolhuis K, Jansen PW. 2019. Executive functioning and neurodevelopmental disorders in early childhood: a prospective population-based study. *Child Adolesc Psychiatry Ment Health*. 13:38.

Pizzagalli F, Auzias G, Yang Q, Mathias SR, Faskowitz J, Boyd J, Amini A, Rivière D, McMahon KL, de Zubicaray GI, *et al*. 2020. The reliability and heritability of cortical folds and their genetic correlations across hemispheres. *Communi Biol*. 3:510.

Pugliese CE, Anthony L, Strang JF, Dudley K, Wallace GL, Kenworthy L. 2015. Increasing adaptive behavior skill deficits from childhood to adolescence in autism Spectrum disorder: role of executive function. *J Autism Dev Disord*. 45:1579–1587.

Rabiee A, Vasaghi-Gharamaleki B, Samadi SA, Amiri-Shavaki Y, Alaghband-Rad J, Seyedin S, Hosseini S. 2018. Impaired nonverbal working memory in high-functioning autism spectrum disorder. *Med J Islam Repub Iran*. 32:107.

Rakic P. 1988. *Specification of cerebral cortical areas*. United States: American Association for the Advancement of Science (AAAS).

Rakic P. 2004. Neuroscience. In: *Genetic control of cortical convolutions*. United States: American Association for the Advancement of Science (AAAS).

Rakic P. 2009. Evolution of the neocortex: a perspective from developmental biology. *Nat Rev Neurosci*. 10:724–735.

Rash BG, Rakic P. 2014. Neuroscience. In: *Genetic resolutions of brain convolutions*. United States: American Association for the Advancement of Science (AAAS).

Sánchez M, Lavigne R, Romero JF, Elósegui E. 2019. Emotion regulation in participants diagnosed with attention deficit hyperactivity disorder, before and after an emotion regulation intervention. *Front Psychol*. 10:1092.

Sandin S, Lichtenstein P, Kuja-Halkola R, Hultman C, Larsson H, Reichenberg A. 2017. The heritability of autism spectrum disorder. *JAMA*. 318:1182–1184.

Shaw P, Kabani NJ, Lerch JP, Eckstrand K, Lenroot R, Gogtay N, Greenstein D, Clasen L, Evans A, Rapoport JL *et al*. 2008. Neurodevelopmental trajectories of the human cerebral cortex. *J Neurosci*. 28:3586–3594.

Sun T, Hevner RF. 2014. Growth and folding of the mammalian cerebral cortex: from molecules to malformations. *Nat Rev Neurosci*. 15:217–232.

Thompson SM, Hammen C, Starr LR, Najman JM. 2014. Oxytocin receptor gene polymorphism (rs53576) moderates the intergenerational transmission of depression. *Psychoneuroendocrinology*. 43:11–19.

Van Essen DC. 1997. A tension-based theory of morphogenesis and compact wiring in the central nervous system. *Nature*. 385:313–318.

Yamagata B, Murayama K, Black JM, Hancock R, Mimura M, Yang TT, Reiss AL, Hoeft F. 2016. Female-specific intergenerational transmission patterns of the human corticolimbic circuitry. *J Neurosci*. 36:1254–1260.

Yehuda R, Daskalakis NP, Bierer LM, Bader HN, Klengel T, Holsboer F, Binder EB. 2016. Holocaust exposure induced intergenerational effects on FKBP5 methylation. *Biol Psychiatry*. 80:372–380.

Yehuda R, Engel SM, Brand SR, Seckl J, Marcus SM, Berkowitz GS. 2005. Transgenerational effects of posttraumatic stress disorder in babies of mothers exposed to the world trade Center attacks during pregnancy. *J Clin Endocrinol Metab*. 90:4115–4118.